

RSC Advances



This is an *Accepted Manuscript*, which has been through the Royal Society of Chemistry peer review process and has been accepted for publication.

Accepted Manuscripts are published online shortly after acceptance, before technical editing, formatting and proof reading. Using this free service, authors can make their results available to the community, in citable form, before we publish the edited article. This *Accepted Manuscript* will be replaced by the edited, formatted and paginated article as soon as this is available.

You can find more information about *Accepted Manuscripts* in the [Information for Authors](#).

Please note that technical editing may introduce minor changes to the text and/or graphics, which may alter content. The journal's standard [Terms & Conditions](#) and the [Ethical guidelines](#) still apply. In no event shall the Royal Society of Chemistry be held responsible for any errors or omissions in this *Accepted Manuscript* or any consequences arising from the use of any information it contains.

**LaPO₄-coated Li_{1.2}Mn_{0.56}Ni_{0.16}Co_{0.08}O₂ as cathode materials with enhanced
Coulombic efficiency and rate capability for lithium ion batteries**

Qingliang Xie¹, Chenhao Zhao², Zhibiao Hu², Qi Huang¹, Cheng Chen¹, Kaiyu Liu^{*1,2}

1 College of Chemistry and Chemical Engineering, Central South University, Changsha 410083, Hunan, China.

2 College of Chemistry & Materials Science, LongYan University, LongYan 364012, Fujian, China.

*Corresponding author

E-mail: kaiyuliu67@263.net

Abstract

In this paper, pristine Li-rich layered oxide $\text{Li}[\text{Li}_{0.2}\text{Mn}_{0.56}\text{Ni}_{0.16}\text{Co}_{0.08}]\text{O}_2$ porous microspheres had been successfully synthesized by an urea combustion method, and then coated with 1.0%, 2.0%, and 3.0 wt% LaPO_4 via a facile chemical precipitation route. The structures and morphologies of both pristine and LaPO_4 coated $\text{Li}_{1.2}\text{Mn}_{0.54}\text{Ni}_{0.16}\text{Co}_{0.08}\text{O}_2$ were performed by X-ray diffractometer (XRD), field-emission scanning electron microscopy (FESEM) and high resolution transmission electron microscope (HR-TEM). XPS data and FESEM demonstrate that the LaPO_4 was successfully coated on the surface of the $\text{Li}[\text{Li}_{0.2}\text{Mn}_{0.56}\text{Ni}_{0.16}\text{Co}_{0.08}]\text{O}_2$ porous microspheres. Especially, the 2 wt% LaPO_4 coated- $\text{Li}[\text{Li}_{0.2}\text{Mn}_{0.56}\text{Ni}_{0.16}\text{Co}_{0.08}]\text{O}_2$ demonstrates the best electrochemical performance. As lithium ion battery cathodes, the 2 wt% LaPO_4 coated sample, compared with the pristine one, has shown significantly improved electrochemical performances: the initial Coulombic efficiency improves from 78.81% to 84.76% at 0.1C and the rate compatibility increased from 70 mAh g^{-1} to a high capacity of 112.73 mAh g^{-1} at a current density of 5C. The analysis of dQ/dV plots and electrochemical impedance spectroscopy (EIS) demonstrate that the enhanced electrochemical performance is mainly attributed to the LaPO_4 coating layer can not only stabilize the cathodes structure by reducing the loss of oxygen, but also protect the Li-rich cathodes from decreasing the side reactions of $\text{Li}[\text{Li}_{0.2}\text{Mn}_{0.56}\text{Ni}_{0.16}\text{Co}_{0.08}]\text{O}_2$ with the electrolyte and lower the charge transfer resistance of the sample.

Introduction

Lithium-ion batteries (LIBs) have been broadly used for portable electronics and expanding rapidly to the field of hybrid electric vehicles (HEVs), plug-in hybrid vehicles (PHEVs), and electric vehicles (EVs). To meet the high energy-density requirements for LIBs, developing a cathode material with high capacity, high operating voltage and good rate capability are becoming more and more imminent¹⁻⁴. To date, Li-rich layered oxides $x\text{Li}_2\text{MnO}_3 \cdot (1-x)\text{LiMO}_2$ ($M = \text{Ni, Co, Mn, Fe, Cr}$, or other combinations) cathode materials have been considered as one of the most promising candidates owing to their extraordinary high theoretical discharge capacity of more than 250 mAh g^{-1} , high operating potential over 3.7 V (*vs.* Li/Li^+) and low cost in comparison with LiCoO_2 and LiFePO_4 ⁵⁻⁸. In the recent years, the studies on the preparation and electrochemical performance of Li-rich cathode materials have been widely reported. However, the commercialization of these cathode materials still faces many challenges. For example, Li-rich layered oxides still suffered from low initial Coulombic efficiency during the first cycle, poor rate capability, severe capacity fade and voltage fading due to the rearrangement of surface structure caused by the activation of Li_2MnO_3 component above 4.5 V , the erosion from the electrolytes, and the structural transformation during cycling⁹⁻¹².

Many efforts have been taken to improve the electrochemical performance of these Li-rich layered oxides $x\text{Li}_2\text{MnO}_3 \cdot (1-x)\text{LiMO}_2$. It has been proved that element doping is an effective strategy to enhance the Li-ion conductivity and stabilizing the structure of lithium-rich layered oxides materials for lithium-ion batteries. Substitutions (such as Ru and Cr) for transition metal ions ($\text{TM} = \text{Mn, Ni and Co}$) and F for O improve the rate capability and reduce the irreversible capacity in the first cycle^{8, 13}. In addition, surface coating or modification has been testified to be another effective way to improve the electrochemical performance of cathode materials for LIBs by suppressing the surface sensitivity of the cathodes materials. Up to now, surface modification with metal oxides, such as Al_2O_3 and TiO_2 , metal fluorides including CaF_2 , AlF_3 and LaF_3 as a coating layer were helpful to improve both the electrochemistry performance including the high initial Coulombic efficiency, excellent rate capability and large discharge capacity, and thermal stabilities²⁻¹⁴⁻¹⁶. Lately, the preparation and surface modification with metal phosphate have attracted much attention due to they are believed to be potentially available active coating materials for cathodes

compounds in LIBs. The formation of Li-metal-P-O solid state electrolyte coating layer for MPO_4 coated cathodes, compared with other Li^+ ion conductor (for instance Al_2O_3 , TiO_2 , MgO_2), is conducive to enhance the stable capability of electrodes during the charge-discharge process¹⁷⁻²⁰. And recent rare earth phosphate also have attracted much interest for many applications because of the special structure of the rare earth element (the different arrangements of 4f electron bring forth abundant energy levels)^{17, 21-23}. Among them, LaPO_4 coating has been reported to improve the rate capability and cycling stability of LiMn_2O_4 and $\text{Li}[\text{Ni}_{0.5}\text{Mn}_{0.3}\text{Co}_{0.2}]\text{O}_2$ by decrease of electrolyte decomposition reaction and dissolution of active materials^{24, 25}. And also LaPO_4 coating can improve the rate capability of LiFePO_4/C due to the coating layer can protect the LiFePO_4 electrode from corrosion and maintain the structural stability of the material²⁶.

In the present study, LaPO_4 is employed as a coating material to enhance the initial Coulombic efficiency and rate capability of $\text{Li}[\text{Li}_{0.2}\text{Mn}_{0.56}\text{Ni}_{0.16}\text{Co}_{0.08}]\text{O}_2$ cathodes. LaPO_4 coated $\text{Li}[\text{Li}_{0.2}\text{Mn}_{0.56}\text{Ni}_{0.16}\text{Co}_{0.08}]\text{O}_2$ is successfully prepared via a facile chemical precipitation route. Experimental results show that electrode of $\text{Li}[\text{Li}_{0.2}\text{Mn}_{0.56}\text{Ni}_{0.16}\text{Co}_{0.08}]\text{O}_2$ coated by 2 wt% LaPO_4 exhibits excellent rate capability and high initial Coulombic efficiency compared with pristine material. In particularly, the effects of coating on the structure and electrochemical properties were investigated in detail.

Experiment

2.1 Preparation of pristine and LaPO₄-coated samples

All raw materials were analytical-grade. Li[Li_{0.2}Mn_{0.56}Ni_{0.16}Co_{0.08}]O₂ was synthesized via a facile urea combustion method. described as follows: 2.602g aqueous solution of Mn(NO₃)₂ (50wt%), 2.196g CO(NH₂)₂, 1.0114g LiNO₃ (5% Li excess), 0.2794 Co(NO₃)₂·6H₂O and 0.5584g Ni(NO₃)₂·6H₂O were dissolved together in 10 ml distilled water to form a uniform solution. Afterwards, the obtained mixed solution was heated in a muffle furnace at 450°C for 40 minutes in air to remove organic contents. Then, the precursors were ground in agate mortar and subsequent calcination in a muffle furnace at 850°C for 10 h under air to gain pure Li[Li_{0.2}Mn_{0.56}Ni_{0.16}Co_{0.08}]O₂, and then cooled down naturally to room temperature.

To prepared LaPO₄-coated Li[Li_{0.2}Mn_{0.56}Ni_{0.16}Co_{0.08}]O₂. Firstly, lanthanum nitrate and ammonium phosphate were dissolved in distill water it is completely reacted, and then the pristine Li[Li_{0.2}Mn_{0.56}Ni_{0.16}Co_{0.08}]O₂ powder was added to the suspension and was magnetically stirred for 30 min to form a slurry. The amount of LaPO₄ in the solution was set as the mass ratios of LaPO₄/Li[Li_{0.2}Mn_{0.56}Ni_{0.16}Co_{0.08}]O₂ =1 wt%, 2 wt% and 3 wt% respectively. The obtained solution was constantly stirred at 80°C until the solvent was evaporated. Afterwards, the wet powder was dried at 80°C in vacuum drying oven until the solvent was completely removed. Finally, the dry powers were further annealed in an argon atmosphere at 450°C for 4h to gain the LaPO₄-coated Li[Li_{0.2}Mn_{0.56}Ni_{0.16}Co_{0.08}]O₂.

2.2 Structure and morphology characterizations

The crystalline structure of the pristine sample and LaPO₄-coated Li[Li_{0.2}Mn_{0.56}Ni_{0.16}Co_{0.08}]O₂ were characterized by X-ray diffractometer (DX-2007 LiaoNing DanDong) within 2 theta range from 10° to 80° at a scanning rate of 0.03°/s. The particle size and morphology of the pristine Li[Li_{0.2}Mn_{0.56}Ni_{0.16}Co_{0.08}]O₂ and LaPO₄ coated Li[Li_{0.2}Mn_{0.56}Ni_{0.16}Co_{0.08}]O₂ were performed using a Quanta FEG 250 field emission scanning electron microscope (FEI, Electron optics, B.V.). The surface state of the obtained products was characterized by X-ray photoelectron spectroscopy (XPS, ESCALAB250). The surface microstructure of coated sample was observed by TEM (JEM-2100F).

2.3 Electrochemical characterization

Electrode slurry was fabricated by mixing active material, polyvinylidene Fluoride (PVDF) binder and acetylene black in the ratio of 80:10:10 together with a certain amount of N-methyl-2

pyrrolidine (NMP) solvent, and then the prepared-slurry was pasted on aluminum foil. After drying at 80°C in a vacuum drying oven the dried aluminum foil were punched into discs with a diameter of 14 mm for assembling the coin cells and the mean mass loading of active materials were controlled between 2.3 and 2.6 mg cm⁻². The coin cell (CR2016) was assembled in an argon-filled glove box, using the prepared-positive electrodes as cathodes and highly pure lithium foils as reference and counter electrode. Celgard 2500 microporous polypropylene membrane was used as separator and Commercial LBC 301 LiPF₆ solution (ShenZhen XinZhouBang) was used as electrolyte. The Galvanic charge and discharge test of assembled cells were performed using NEWARE battery test systems in a range voltage with 2.0-4.7V at room temperature and 55°C. Electrochemical impedance spectroscopy (EIS) study was performed using an electrochemical workstation (CHI660D, ShangHai ChenHua) in a frequency range of 0.01MHz to 0.1MHz. Plots of dQ/dV vs. voltage were calculated based on the testing data of charge/discharge.

Result and discussion

3.1 Structure and morphology of pristine and LaPO₄-coated Li[Li_{0.2}Mn_{0.56}Ni_{0.16}Co_{0.08}]O₂

XRD patterns of Li[Li_{0.2}Mn_{0.56}Ni_{0.16}Co_{0.08}]O₂ before and after LaPO₄ modifications are shown in Fig. 1. All the sharp diffraction peaks can be indexed to a hexagonal α-NaFeO₂ type structure with a space group R-3m^{27, 28}. Adjacent peaks of (006)/(012) and (108)/(110) were divided clearly, indicating that well crystalline layered structure are obtained of all samples. Weak XRD peaks observed within 2 degree of 2θ and 25° suggest the periodic occupation of Li⁺ ions in the transition metal layers of crystalline LiMO₂, and the resulting LiMn-typed cation arrangements indicate the coexistence of both crystalline Li₂MnO₃ (also referred to as layered Li(Li_{1/3}Mn_{2/3})O₂) and LiNi_{0.4}Co_{0.2}Mn_{0.4}O₂)^{19, 29, 30}. Based on these results, no LaPO₄ and other impurities diffraction peaks can be observed in the XRD pattern and the bulk structure of the Li[Li_{0.2}Mn_{0.56}Ni_{0.16}Co_{0.08}]O₂ remains unchanged after surface coating process may due to the low content of LaPO₄, indicating the coated LaPO₄ has little influence on the bulk structure of the pristine sample.

The particle size and morphology of the pristine Li[Li_{0.2}Mn_{0.56}Ni_{0.16}Co_{0.08}]O₂ and 2 wt% LaPO₄ coated Li[Li_{0.2}Mn_{0.56}Ni_{0.16}Co_{0.08}]O₂ were investigated by scanning electron microscope (SEM) and transmission electron microscope (TEM), as demonstrated in Fig. 2 . It can be clearly seen that the bare Li[Li_{0.2}Mn_{0.56}Ni_{0.16}Co_{0.08}]O₂ was composed of porous microspheres, and these microspheres

constructed by numerous nanoparticles that have a particle size distributed from 3 to 5 μm in Fig. 2a and b. As we know, the cathode materials with porous microspheres structure would be very suitable for a lithium ion battery. Firstly, the porous microspheres of the pristine sample will have excellent cycling stability during the charge-discharge process due to stable three-dimension framework. Secondly, the numerous nanoparticles which aggregate to form porous microspheres help to transmission of Li ions by providing a short path for the intercalation/deintercalation of lithium ions. Therefore, the electrochemical performance of the $\text{Li}[\text{Li}_{0.2}\text{Mn}_{0.56}\text{Ni}_{0.16}\text{Co}_{0.08}]\text{O}_2$ would be worth expecting after coated with functional materials LaPO_4 . SEM image of 2 wt% LaPO_4 -coated $\text{Li}[\text{Li}_{0.2}\text{Mn}_{0.56}\text{Ni}_{0.16}\text{Co}_{0.08}]\text{O}_2$ was shown in Fig. 2c, compared with the pristine sample (Fig. 2b), a bright coating layer could be observed on the surface of coated sample, and the space between nanoparticles is less differentiate due to the existence of the coating layer. The surface morphologies and microstructure for 2 wt% LaPO_4 coated samples are further analysis by typical high resolution TEM (HRTEM) observations as shown in Fig. 2d. A clear lattice fringe with a spacing of 0.47 nm in the surface of nanoparticles can be assigned to the (003) crystal face of $\text{Li}[\text{Li}_{0.2}\text{Mn}_{0.56}\text{Ni}_{0.16}\text{Co}_{0.08}]\text{O}_2$. And the 2% LaPO_4 coated $\text{Li}[\text{Li}_{0.2}\text{Mn}_{0.56}\text{Ni}_{0.16}\text{Co}_{0.08}]\text{O}_2$ particles are covered with a thin layer and the thickness of the coating layer was calculated about 10-12 nm. This thin LaPO_4 coating layer will segregate the direct contact between the electrode and electrolyte and thus reduce the side reactions between the active material and electrolyte to some extent.

Furthermore, the selected area energy dispersive spectroscopic (EDS) image and corresponding element analysis of 2 wt% LaPO_4 -coated $\text{Li}[\text{Li}_{0.2}\text{Mn}_{0.56}\text{Ni}_{0.16}\text{Co}_{0.08}]\text{O}_2$ is shown in Fig.3. The calculated element ratio of Mn: Ni: Co in Fig. 3 should be 0.568: 0.164: 0.0795, which is much close to the chemical formula of $\text{Li}[\text{Li}_{0.2}\text{Mn}_{0.56}\text{Ni}_{0.16}\text{Co}_{0.08}]\text{O}_2$ (i. e., 0.560 : 0.160 : 0.08). The calculated atomic ratio of La: Mn is 1.0: 30.1 from the EDS analysis, and the theoretical data based on 2 wt% LaPO_4 coating should be 1.0: 28.0. These results indicate that the actual element composition of as-prepared pristine and 2 wt% LaPO_4 -coated sample is well consistent with the original experimental project. It should be emphasized that the content of O and P is difficult to be accurately detected by EDS. However, the EDS image also shows the coexistence of O and P element.

X-ray photoelectron spectroscopy is a commonly used method to study the electronic structure of the materials due to the XPS binding energies can provide useful information on the oxidation state of different elements in materials. The XPS spectrums of bare and 2 wt% LaPO_4 -coated

Li[Li_{0.2}Mn_{0.56}Ni_{0.16}Co_{0.08}]O₂ are carried out as shown in Fig. 4. The characteristic binding energies of P2p and La3d are 132.99 eV and 834.89 eV, respectively, which are in accordance with those of pure LaPO₄²⁴. Compared with the bare Li[Li_{0.2}Mn_{0.56}Ni_{0.16}Co_{0.08}]O₂, the Ni2p and Mn2p peaks of LaPO₄-coated Li[Li_{0.2}Mn_{0.56}Ni_{0.16}Co_{0.08}]O₂ have no obvious chemical shift, indicating that the Ni and Mn ion environments in the structure have not been changed^{31, 32}. However, the intensity of each peak decreases obviously after coating, which is attributed to the formation of the LaPO₄ layer on the surface of Li[Li_{0.2}Mn_{0.56}Ni_{0.16}Co_{0.08}]O₂. Combining the EDS pattern, XRD pattern and XPS test results, we can conclude that the LaPO₄ have been successfully coated on the surface of the aimed material.

The initial charge-discharge curves of uncoated and LaPO₄ coated (1.0%, 2.0% and 3.0 wt%) Li[Li_{0.2}Mn_{0.56}Ni_{0.16}Co_{0.08}]O₂ cathodes materials at a discharge rate of 0.1C in the voltage range of 2.0 - 4.7V at room temperature(25°C) are shown in Fig.5a. In this figure, all the electrodes show smooth charge/ discharge slopes, indicating the bulk structure of Li[Li_{0.2}Mn_{0.56}Ni_{0.16}Co_{0.08}]O₂ have no significant change happens after surface modification with different content of LaPO₄. As we all know, the typical Li-rich layered oxides have two distinct charge plateaus during cycling. One at the about 4.0 V is corresponding to the Li-extraction from the structure of space group R-3m accompanying with the oxidation of mainly Ni²⁺/Ni⁴⁺^{5, 28, 33, 34}. The other one plateau above 4.5 V represents the activation of the Li₂MnO₃-like region, which is irreversible and only appears in the initial cycle^{35, 36}. As is well-known, one of the significant drawbacks of lithium rich layered oxides cathodes is the tremendous irreversible capacity loss of about 40-100 mAh g⁻¹ in the initial charge-discharge process. And the Li⁺ in the Li₂MnO₃-like region will be extracted at about 4.5 V accompanying with the loss of O, which is the main reason of leading to the irreversible capacity loss and induce the diffusion of transition metal ions from surface to bulk where they occupy vacancies by Li removal^{35, 37}. The electrochemical inactive Li₂MnO₃ region became active mainly due to the removing of Li₂O from the lattice and forming of [MnO₂]^{21, 38}. As reported by many literature, the surface modification could reduce the activity of extracted oxygen, enhancing the reversible prosperities for lithium rich layered oxides cathodes^{39, 40}. As shown in fig.5a, the initial charge/discharge capacity of the pristine, 1.0, 2.0 and 3 wt% LaPO₄-coated Li-rich materials are 325.3/256.4, 333.4/278.8, 328.1/278.1 and 317.3/259.8 mAh g⁻¹, give a Coulombic efficiency of 78.81, 83.64, 84.76 and 81.88%, respectively. It's clear that the irreversible capacity loss of the

pristine, 1.0, 2.0 and 3 wt% LaPO₄-coated Li-rich materials are 68.9, 54.6, 50 and 57.5 mAh g⁻¹. It can be seen that a suitable content of LaPO₄ (2 wt%) coated on Li-rich samples can effectively improve the initial Coulombic efficiency of Li-rich cathodes materials and reduce the irreversible capacity loss in the first cycle process, implying a huge improvement on the electrodes structure stability. The main reason of the relatively lower irreversible capacity loss and higher initial coulombic efficiency for the LaPO₄-coated cathode can be attributed to the LaPO₄ coating layer can be regarded as a buffer layer to promote the formation of inactive O₂ molecules, preventing the side reaction of electrolyte oxidation caused by active oxygen species. And the successful surface coating with LaPO₄ can also suppress the dissolution of the transition metals.

Figure 5(b) is dQ/dV plots of the electrochemical data shown in Figures 5(a). During the first charge process, the peak potential arises around 4.6V (vs Li/Li⁺), this is consistent with the appearance of the long potential plateau due to irreversible loss of oxygen as Li₂O removal from the layered lattice during the initial charging. According to the result of dQ/dV plots in Figure 5(b), the 2 wt% LaPO₄-coated Li[Li_{0.2}Mn_{0.56}Ni_{0.16}Co_{0.08}]O₂, compared with the pristine sample, has a high discharge voltage, which demonstrate the LaPO₄ coating layer can decrease the polarization to some extent.

The cycling performance and discharge capacity of the electrode materials at a high current density is still important parameters for lithium battery. The first charge-discharge curves of pristine, 1.0%, 2.0% and 3.0 wt% LaPO₄ coated Li[Li_{0.2}Mn_{0.56}Ni_{0.16}Co_{0.08}]O₂ at a current density of 1C in room temperature(25°C) were performed in Fig. 6a, the initial charge/discharge capacity of the pristine, 1.0, 2.0 and 3 wt% LaPO₄-coated Li-rich materials are 243.6/170.9, 241.4/177.6, 240.6/177.6 and 235.9/175.0 mAh g⁻¹, give a Coulombic efficiency of 70.16, 73.58, 78.84 and 74.17%, respectively. It can be seen that the LaPO₄ coated Li[Li_{0.2}Mn_{0.56}Ni_{0.16}Co_{0.08}]O₂ exhibits higher initial Coulombic efficiency than the pristine samples. Especially the 2.0 wt% LaPO₄ has the extraordinary high initial Coulombic efficiency of 78.84% compared with the pristine samples (70.16%) at current density of 1C. The influence of LaPO₄ coating layer on the capacity retention of Li-rich cells in a potential region between 2.0 and 4.7V at 1 C in room temperature(25°C) is shown in Fig. 6(b). The capacity retention of 2 wt% LaPO₄ coated sample, compared with the pristine sample with capacity retention of 86.4%, has increased to 89.3% after 50 cycles. The improvements herein can be attributed to the LaPO₄ coating layer, which can not only protect the electrode from the

erosion from the electrolyte but also stabilize the cathodes structure by decreasing the loss of oxygen.

In order to study the thermal stability of the pristine $\text{Li}_{1.2}\text{Mn}_{0.56}\text{Ni}_{0.16}\text{Co}_{0.08}\text{O}_2$ and 2% LaPO_4 coated $\text{Li}_{1.2}\text{Mn}_{0.56}\text{Ni}_{0.16}\text{Co}_{0.08}\text{O}_2$. Fig.S1 show the capacity retention of the pristine $\text{Li}_{1.2}\text{Mn}_{0.56}\text{Ni}_{0.16}\text{Co}_{0.08}\text{O}_2$ and 2% LaPO_4 coated $\text{Li}_{1.2}\text{Mn}_{0.56}\text{Ni}_{0.16}\text{Co}_{0.08}\text{O}_2$ cathodes at 55°C in a potential region between 2.0 and 4.7V at 1 C. After 30 cycles, the capacity of the pristine $\text{Li}_{1.2}\text{Mn}_{0.56}\text{Ni}_{0.16}\text{Co}_{0.08}\text{O}_2$ rapidly fades to 140 mAhg⁻¹, with the low capacity retention of 77.34%. However, the 2% LaPO_4 coated $\text{Li}_{1.2}\text{Mn}_{0.56}\text{Ni}_{0.16}\text{Co}_{0.08}\text{O}_2$ still keeps a quite high capacity of 184 mAh g⁻¹, and the capacity retention is as high as 89.71%. And the DSC curves of the $\text{Li}_{1.2}\text{Mn}_{0.56}\text{Ni}_{0.16}\text{Co}_{0.08}\text{O}_2$ before and after the surface modification with 2 % LaPO_4 after charging to 4.7 V (vs Li/Li⁺) in the first cycle was shown in Fig.S2. The onset temperature of the modified sample with 2% LaPO_4 nanoparticles is 212.76 °C, higher than that (203.5 °C) of the pristine sample, indicating the improved thermal stability of the cathode by the surface modification with LaPO_4 nanoparticles. Therefore, it can be concluded that the coated LaPO_4 layer can protect the active material from dissolving into the electrolyte at elevated temperature, and improve the high-temperature cycling stability of Li-rich electrodes.

Rate capability is also a very important parameter in judging their use in practical lithium ion batteries. It have been widely reported that one of the most important drawback of Li-rich layered oxides is poor rate capability, which impeding the commercialization of this material. The LaPO_4 coating layer may improve the C-rates of the coated samples because the phosphate coating layer can not only facilitate the charge transfer between the electrode and electrolyte, but also prevent direct contact of the active material with the electrolyte resulting in the decrease of electrolyte decomposition reactions and dissolution of active materials. Fig. 7 shows the rate discharging capacities of all the samples at the applied current densities. The cells were charged galvanostatically with a current density of 0.1 C (20 mA g⁻¹) before each discharge and were then discharged at a C rate from 0.5 C to 5C. As observed in Fig. 7, the discharge capacities gradually decrease with increasing the charge-discharge current. Meanwhile, it is clearly observed that all the LaPO_4 coated samples have better rate capability than the pristine sample, especially at high rates. Obviously, the rate capability of $\text{Li}[\text{Li}_{0.2}\text{Mn}_{0.56}\text{Ni}_{0.16}\text{Co}_{0.08}]\text{O}_2$ are greatly improved with the appropriate LaPO_4 coating amount of 2%. Furthermore, the discharge capacity can be completely recovered when the current density is reset to 0.5C, indicating that the LaPO_4 -coated $\text{Li}[\text{Li}_{0.2}\text{Mn}_{0.56}\text{Ni}_{0.16}\text{Co}_{0.08}]\text{O}_2$

electrodes has a desirable electrochemical reversibility and structure stability.

EIS test was carried out to further understand the LaPO₄ coating effect on charge–discharge process. Fig. 8 shows the electrochemical impedance spectroscopy (EIS) of the pristine and 2 wt% LaPO₄-coated Li[Li_{0.2}Mn_{0.56}Ni_{0.16}Co_{0.08}]O₂, collected after 3 charge-discharge cycles at 0.1C. Each of the plots consist of a semicircle in the high-frequency region and a slope in the low frequency region, in which the high-frequency semicircle is related to the charge transfer resistance (R_{ct}) in the electrode/electrolyte and the low-frequency slope line on behalf of the impedance of the lithium ion diffusion in bulk electrode materials^{41, 42}. It can be clearly seen that the results show obviously decreased R_{ct} values after LaPO₄ coating. The R_{ct} value of the pristine cathode is 210.8 Ω while the LaPO₄-coated cathodes show much smaller R_{ct} value about 161.5 Ω. Therefore, it can be concluded that the improvement of the LaPO₄ on the electrochemical performance of the Li[Li_{0.2}Mn_{0.56}Ni_{0.16}Co_{0.08}]O₂ is mainly attributed to the LaPO₄ coating layer not only reduce the side reaction of Li[Li_{0.2}Mn_{0.56}Ni_{0.16}Co_{0.08}]O₂ with the electrolyte, but also increase the Li⁺ migration rate at the interface.

Conclusion

In this paper, LaPO₄ was uniformly coated on the surface of the Li-rich layered oxides Li[Li_{0.2}Mn_{0.56}Ni_{0.16}Co_{0.08}]O₂ porous microspheres via a facile chemical precipitation route. The LaPO₄ coating layer can not only protect the materials against the erosion from the electrolytes, but also increase the Li⁺ migration rate at the interface. As a result, the 2 wt% LaPO₄ coated Li[Li_{0.2}Mn_{0.56}Ni_{0.16}Co_{0.08}]O₂ exhibits enhanced initial Coulombic efficiency and rate capability compared to the pristine one. Therefore, we conclude that an appropriate LaPO₄ coating is an effective method to overcome the main existing problems of Li-rich layered oxides Li[Li_{0.2}Mn_{0.56}Ni_{0.16}Co_{0.08}]O₂ cathode material for high power applications.

Acknowledgements

This work was financially supported by the Science and Technology Program of LongYan (2014LY36) and the School Research Program of LongYan University (LC2013008).

References

1. J. Liu, Q. Wang, B. Reeja-Jayan and A. Manthiram, *Electrochem. Commun.*, 2010, **12**, 750-753.
2. C. Lu, H. Wu, Y. Zhang, H. Liu, B. Chen, N. Wu and S. Wang, *J. Power Sources*, 2014, **267**, 682-691.
3. J. B. Goodenough and K. S. Park, *J. Am. Chem. Soc.*, 2013, **135**, 1167-1176.
4. F. Dang, T. Hoshino, Y. Oaki, E. Hosono, H. Zhou and H. Imai, *Nanoscale*, 2013, **5**, 2352-2357.
5. H.-J. Kim, H.-G. Jung, B. Scrosati and Y.-K. Sun, *J. Power Sources*, 2012, **203**, 115-120.
6. J. Li, L. Wang, L. Wang, J. Luo, J. Gao, J. Li, J. Wang, X. He, G. Tian and S. Fan, *J. Power Sources*, 2013, **244**, 652-657.
7. D. Mohanty, S. Kalnaus, R. A. Meisner, K. J. Rhodes, J. Li, E. A. Payzant, D. L. Wood and C. Daniel, *J. Power Sources*, 2013, **229**, 239-248.
8. J. W. Min, J. Gim, J. Song, W.-H. Ryu, J.-W. Lee, Y.-I. Kim, J. Kim and W. B. Im, *Electrochim. Acta*, 2013, **100**, 10-17.
9. Z. Lu and J. R. Dahn, *J. Electrochem. Soc.*, 2002, **149**, A815-A822.
10. S. Kim, C. Kim, Y.-I. Jhon, J.-K. Noh, S. H. Vemuri, R. Smith, K. Y. Chung, M. S. Jhon and B.-W. Cho, *J. Mater. Chem.*, 2012, **22**, 25418.
11. D. I. Choi, H. Lee, D. J. Lee, K.-W. Nam, J.-S. Kim, R. A. Huggins, J.-K. Park and J. W. Choi, *J. Mater. Chem. A.*, 2013, **1**, 5320.
12. C. Yu, G. Li, X. Guan, J. Zheng, L. Li and T. Chen, *Electrochimica Acta*, 2012, **81**, 283-291.
13. L. F. Jiao, M. Zhang, H. T. Yuan, M. Zhao, J. Guo, W. Wang, X. D. Zhou and Y. M. Wang, *J. Power Sources*, 2007, **167**, 178-184.
14. Y. K. Sun, M. J. Lee, C. S. Yoon, J. Hassoun, K. Amine and B. Scrosati, *Adv. Mater.*, 2012, **24**, 1192-1196.
15. X.-H. Liu, L.-Q. Kou, T. Shi, K. Liu and L. Chen, *J. Power Sources*, 2014, **267**, 874-880.
16. Q. Xie, Z. Hu, C. Zhao, S. Zhang and K. Liu, *RSC Adv.*, 2015, **5**, 50859-50864.
17. H. Z. Zhang, Q. Q. Qiao, G. R. Li and X. P. Gao, *J. Mater. Chem. A.*, 2014, **2**, 7454.
18. J. M. Zheng, J. Li, Z. R. Zhang, X. J. Guo and Y. Yang, *Solid State Ionics*, 2008, **179**, 1794-1799.
19. Y. J. Kang, J. H. Kim, S. W. Lee and Y. K. Sun, *Electrochim. Acta.*, 2005, **50**, 4784-4791.
20. D.-J. Lee, B. Scrosati and Y.-K. Sun, *J. Power Sources*, 2011, **196**, 7742-7746.
21. X. Liu, H. Li, E. Yoo, M. Ishida and H. Zhou, *Electrochim. Acta.*, 2012, **83**, 253-258.
22. Q. Q. Qiao, H. Z. Zhang, G. R. Li, S. H. Ye, C. W. Wang and X. P. Gao, *J. Mater. Chem. A.*, 2013, **1**, 5262.
23. C. Wu, X. Fang, X. Guo, Y. Mao, J. Ma, C. Zhao, Z. Wang and L. Chen, *J. Power Sources*, 2013, **231**, 44-49.
24. H. G. Song, K.-S. Park and Y. J. Park, *Solid State Ionics*, 2012, **225**, 532-537.
25. P. Mohan and G. Paruthimal Kalaignan, *Ceram. Int.*, 2014, **40**, 1415-1421.
26. Z. Ma, Y. Peng, G. Wang, Y. Fan, J. Song, T. Liu, X. Qin and G. Shao, *Electrochim. Acta.*, 2015, **156**, 77-85.
27. S. J. Shi, J. P. Tu, Y. Y. Tang, X. Y. Liu, X. Y. Zhao, X. L. Wang and C. D. Gu, *J. Power Sources*, 2013, **241**, 186-195.

28. X. Zhang, S. Sun, Q. Wu, N. Wan, D. Pan and Y. Bai, *J. Power Sources*, 2015, **282**, 378-384.
29. D. K. Lee, S. H. Park, K. Amine, H. J. Bang, J. Parakash and Y. K. Sun, *J. Power Sources*, 2006, **162**, 1346-1350.
30. J. Liu and A. Manthiram, *J. Mater. Chem.*, 2010, **20**, 3961.
31. S. Zhao, Y. Bai, L. Ding, B. Wang and W. Zhang, *Solid State Ionics*, 2013, **247-248**, 22-29.
32. J.-L. Liu, J. Wang and Y.-Y. Xia, *Electrochim. Acta.*, 2011, **56**, 7392-7396.
33. Q. Y. Wang, J. Liu, A. V. Murugan and A. Manthiram, *J. Mater. Chem.*, 2009, **19**, 4965.
34. S. J. Shi, J. P. Tu, Y. Y. Tang, Y. X. Yu, Y. Q. Zhang, X. L. Wang and C. D. Gu, *J. Power Sources*, 2013, **228**, 14-23.
35. M. Oishi, T. Fujimoto, Y. Takanashi, Y. Orikasa, A. Kawamura, T. Ina, H. Yamashige, D. Takamatsu, K. Sato, H. Murayama, H. Tanida, H. Arai, H. Ishii, C. Yogi, I. Watanabe, T. Ohta, A. Mineshige, Y. Uchimoto and Z. Ogumi, *J. Power Sources*, 2013, **222**, 45-51.
36. D. Mohanty, A. S. Sefat, S. Kalnaus, J. Li, R. A. Meisner, E. A. Payzant, D. P. Abraham, D. L. Wood and C. Daniel, *Journal of Materials Chemistry A*, 2013, **1**, 6249.
37. E.-S. Lee and A. Manthiram, *J. Mater. Chem. A.*, 2014, **2**, 3932.
38. F. Li, S.-X. Zhao, K.-Z. Wang, B.-H. Li and C.-W. Nan, *Electrochim. Acta.*, 2013, **97**, 17-22.
39. T. Shi, Y. Dong, C.-M. Wang, F. Tao and L. Chen, *J. Power Sources*, 2015, **273**, 959-965.
40. B. Liu, Q. Zhang, S. He, Y. Sato, J. Zheng and D. Li, *Electrochim. Acta.*, 2011, **56**, 6748-6751.
41. D.-J. Lee, K.-S. Lee, S.-T. Myung, H. Yashiro and Y.-K. Sun, *J. Power Sources*, 2011, **196**, 1353-1357.
42. Y. Bai, K. Jiang, S. Sun, Q. Wu, X. Lu and N. Wan, *Electrochim. Acta.*, 2014, **134**, 347-354.

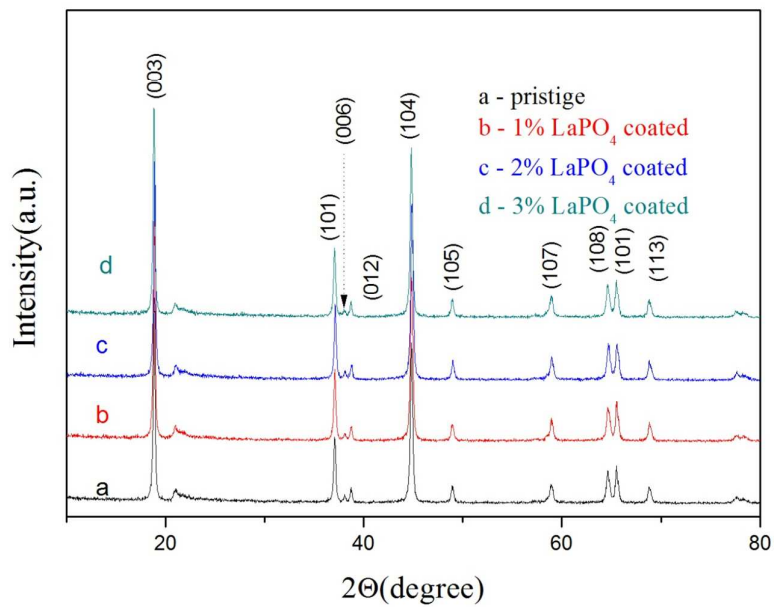


Fig.1. XRD pattern of as-prepared pristine and LaPO₄-coated Li[Li_{0.2}Mn_{0.56}Ni_{0.16}Co_{0.08}]O₂.

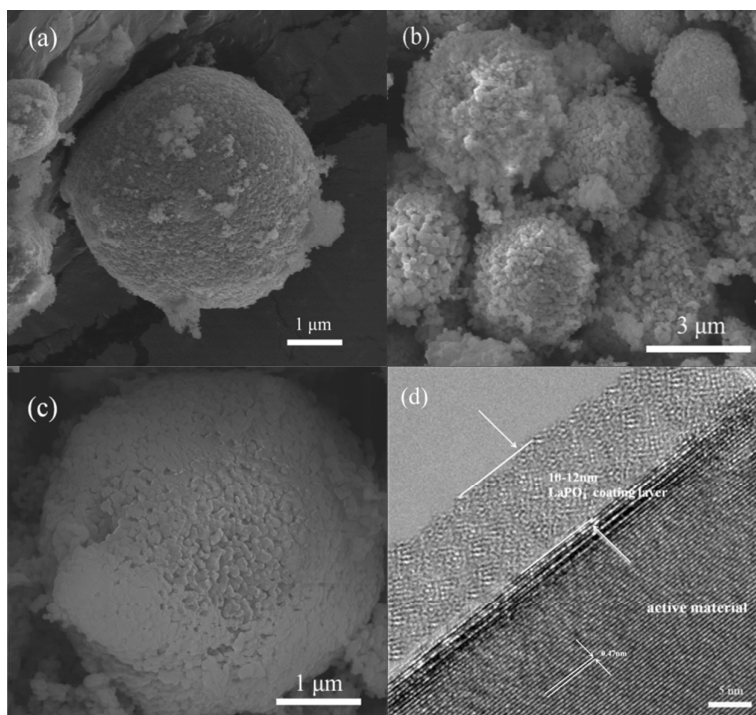


Fig. 2 SEM images of the pristine $\text{Li}[\text{Li}_{0.2}\text{Mn}_{0.56}\text{Ni}_{0.16}\text{Co}_{0.08}]\text{O}_2$ at (a) low magnification and (b) high magnification, (c) 2 wt% LaPO_4 -coated $\text{Li}[\text{Li}_{0.2}\text{Mn}_{0.56}\text{Ni}_{0.16}\text{Co}_{0.08}]\text{O}_2$ and (d) HR-TEM and SAED (selected area electron diffraction) image of the LaPO_4 -coated $\text{Li}[\text{Li}_{0.2}\text{Mn}_{0.56}\text{Ni}_{0.16}\text{Co}_{0.08}]\text{O}_2$.

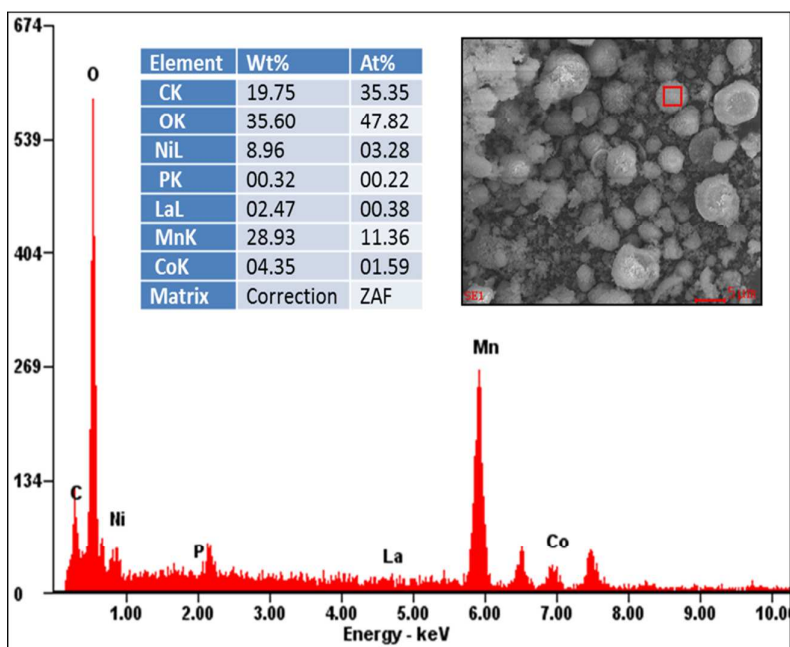


Fig. 3 Element dispersive spectrum (EDS) of 2 wt% LaPO_4 -coated $\text{Li}[\text{Li}_{0.2}\text{Mn}_{0.56}\text{Ni}_{0.16}\text{Co}_{0.08}]\text{O}_2$. The insets are the selected area image and detailed elemental analysis.

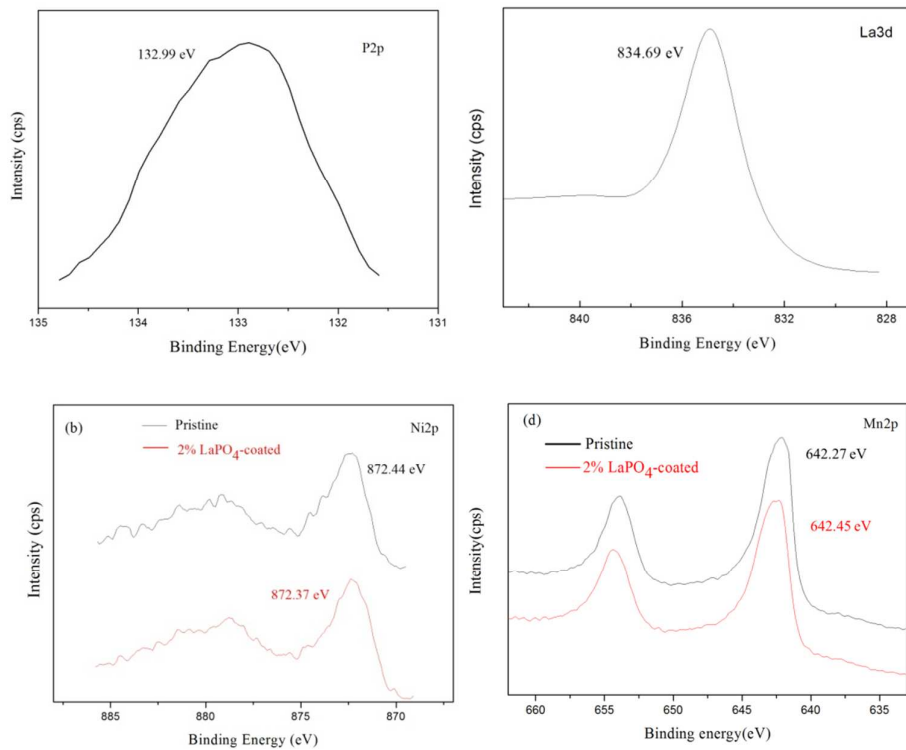


Fig. 4 XPS spectra of bare and 2wt% LaPO₄-coated Li[Li_{0.2}Mn_{0.56}Ni_{0.16}Co_{0.08}]O₂ (a) P2p, (b) La3d, (c) Ni2p and (d) Mn2p.

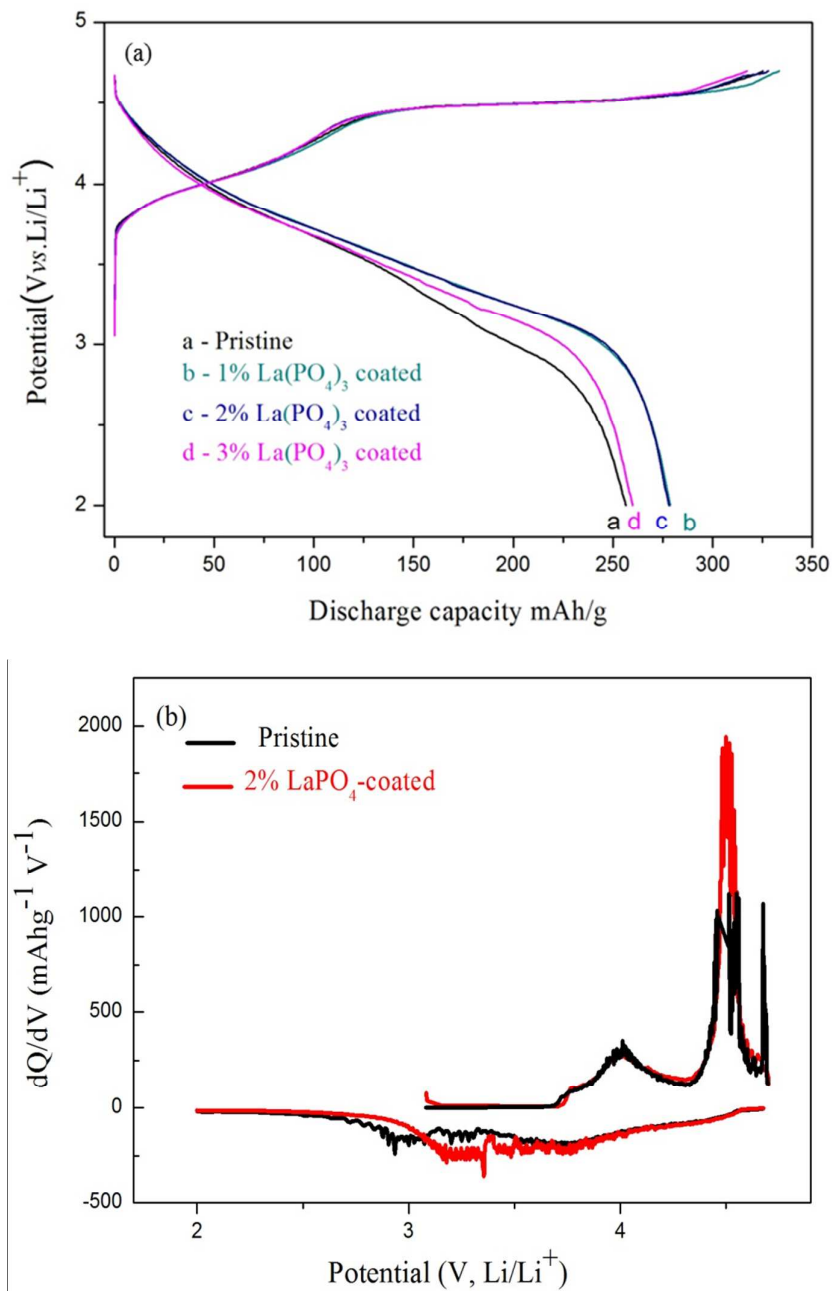


Fig. 5 The initial charge–discharge voltage profiles and corresponding differential capacity (dQ/dV) curves for the pristine $\text{Li}[\text{Li}_{0.2}\text{Mn}_{0.56}\text{Ni}_{0.16}\text{Co}_{0.08}]\text{O}_2$ and LaPO_4 -coated $\text{Li}[\text{Li}_{0.2}\text{Mn}_{0.56}\text{Ni}_{0.16}\text{Co}_{0.08}]\text{O}_2$ electrodes at a current density of 0.1 C between 2.0 and 4.7 V.

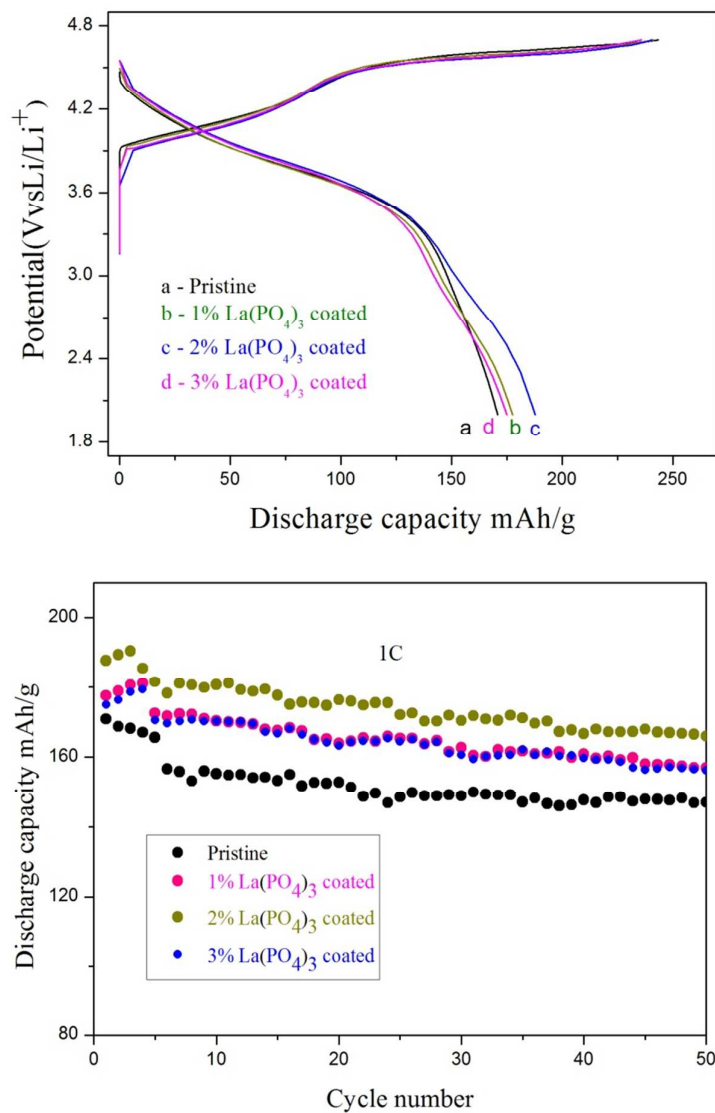


Fig. 6 (a) The initial charge–discharge curves and (b) cycling performance of the $\text{Li}[\text{Li}_{0.2}\text{Mn}_{0.56}\text{Ni}_{0.16}\text{Co}_{0.08}]\text{O}_2$ and LaPO_4 -coated $\text{Li}[\text{Li}_{0.2}\text{Mn}_{0.56}\text{Ni}_{0.16}\text{Co}_{0.08}]\text{O}_2$ electrodes within 2.0–4.7 V at 1 C.

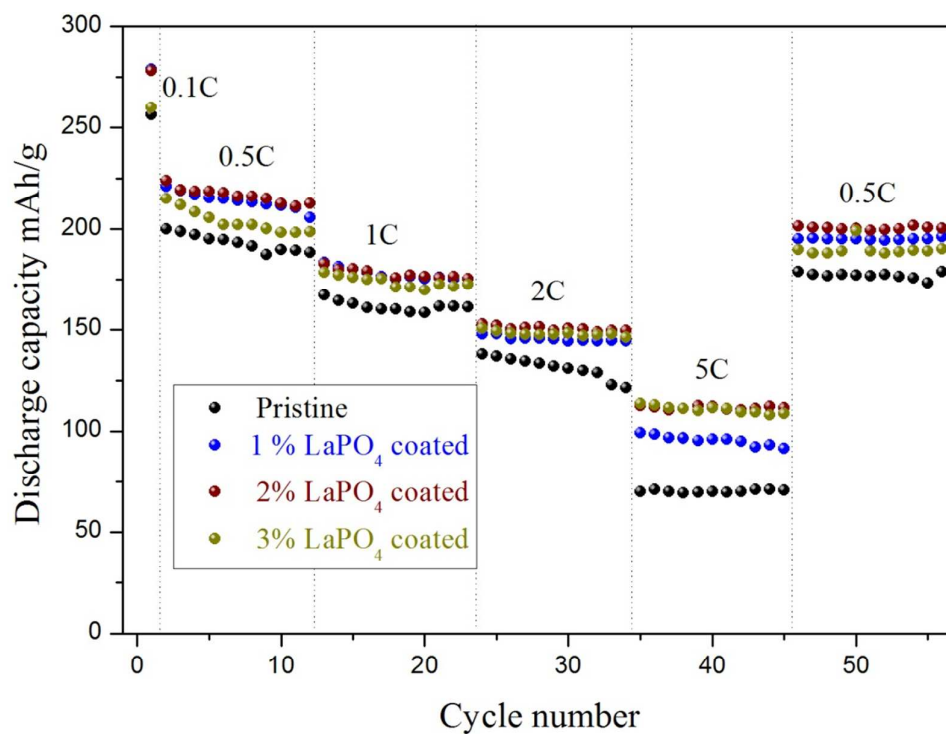


Fig.7 Rate capability of the pristine $\text{Li}[\text{Li}_{0.2}\text{Mn}_{0.56}\text{Ni}_{0.16}\text{Co}_{0.08}]\text{O}_2$ and LaPO_4 -coated $\text{Li}[\text{Li}_{0.2}\text{Mn}_{0.56}\text{Ni}_{0.16}\text{Co}_{0.08}]\text{O}_2$ electrodes.

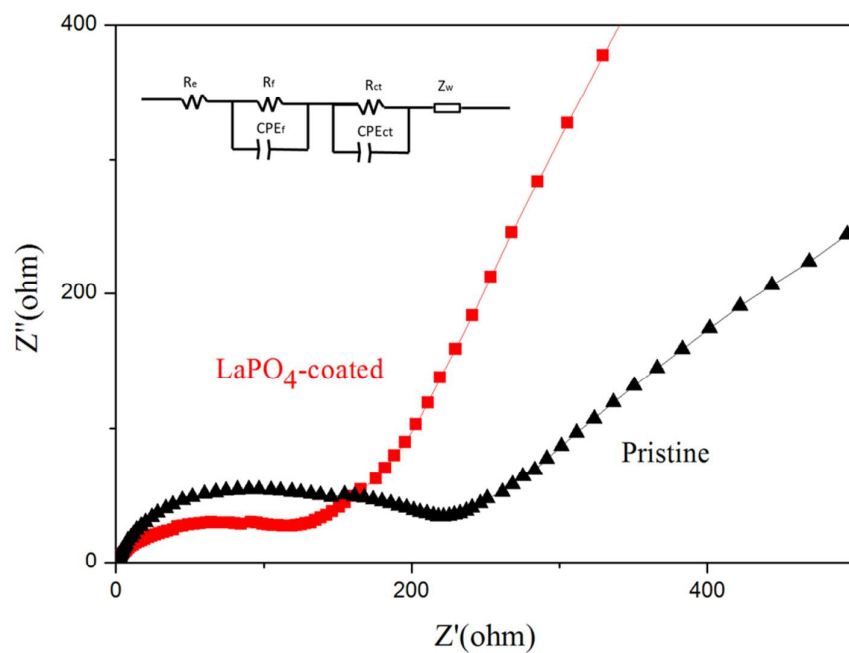


Fig. 8 Electrochemical impedance spectroscopy (EIS) and the equivalent circuit used (inset) for the pristine and LaPO₄-coated Li[Li_{0.2}Mn_{0.56}Ni_{0.16}Co_{0.08}]O₂ after 3 cycles before charging.